

## Transient Voltage-Current Characteristics: New Insights into Plasma Electrolytic Oxidation Process of Aluminium Alloy

Hongping Duan<sup>1,3</sup>, Yunchao Li<sup>2</sup>, Yuan Xia<sup>1,\*</sup>, Shaohua Chen<sup>1</sup>

<sup>1</sup> Institute of Mechanics, Chinese Academy of Sciences, No. 15, Beisihuanxi Road, Beijing 100190, China

<sup>2</sup> Department of Chemistry, Beijing Normal University, No. 19, Xijiekouwai Street, Beijing 100875, China

<sup>3</sup> Naton Institute of Medical Technology, Naton Medical Group, No. 103, Beiqing Road, Beijing 100095, China

\*E-mail: [xia@imech.ac.cn](mailto:xia@imech.ac.cn)

Received: 23 December 2011 / Accepted: 3 July 2012 / Published: 1 August 2012

---

In order to clarify the electrochemical mechanism of plasma electrolytic oxidation (PEO), SEM, Mott-Schottky measurement, and the transient voltage and current (V-I) characteristics were utilized to systematically investigate conductive properties and reaction process of aluminium electrodes. Results indicated that the aluminium electrode coated with oxide coatings exhibited n-type semi-conductive properties and it had a Schottky barrier diode (SBD)-typed structure with the rectification effect on current. These made the transient I-V characteristics have different behaviors in loading and unloading branch of the anodic region during PEO process of aluminium alloy electrode. Moreover, in-situ monitoring on the whole PEO process discovered that the resistance of PEO coatings in anodic and cathodic directions were both increased as treatment time prolonged. These methods and results reported in this paper would offer some new insights into the mechanism of PEO technique.

---

**Keywords:** Plasma electrolytic oxidation; Aluminium; Transient V-I characteristics; Semiconducting properties; Schottky Barrier Diode.

### 1. INTRODUCTION

Plasma electrolytic oxidation (PEO) is a promising and environment-friendly surface treatment technique to fabricate ceramic coatings on valve metals (Al, Mg, Ti etc.) [1]. The ceramic coatings show special properties such as strong adhesion, high hardness, and improved corrosion and wear resistance [2-5]. Therefore, the applications of PEO technique have attracted extensive attentions in aerospace, automotive, textiles and some potential fields.

So far, the fabrication, structures and properties of PEO coatings have been well-investigated, but the growth mechanism of PEO coatings has not been fully clarified. Some researchers have obtained useful information based on the characteristics of PEO process (such as gas evolution, spark discharge, melting and solidification). For example, phenomena of micro-discharge were photographed by high speed camera [6-8], and the density and intensity of spark discharge during PEO process were obtained. Moreover, the optical emission spectroscopy was used to identify species that participate in PEO reactions [9, 10]. The current and voltage behaviors, which can in-situ reflect the properties and reaction process of a general electrode system, have been widely studied to reveal the anodic oxidation mechanism of valve metals [11, 12]. However, it is a technical challenge to in-situ investigate the electrochemical mechanism of a PEO process which was performed under high current and voltage conditions accompanied with numerous transient spark discharge and complicated physical, chemical and plasma reactions. Moreover, in-situ investigation on the electrode reactions during PEO process is difficult because of existence of ceramic oxide coatings on substrate, which makes the aluminium electrode exhibit different electrochemical behavior in comparison with bare metal electrode, but similar to that of semi-conductive or insulating electrode [13]. Recently, the effect of electric signal on coatings properties were characterized by the current/voltage-time behavior [7, 14]. Moreover, the PEO process was investigated preliminarily by our group based on the transient voltage and current (V-I) characteristics that obtained by a signal acquisition system [15]. Unfortunately, the correlation of the V-I characteristics, reactions and conductive properties of electrode systems have not been revealed. So, detailed analysis of the conducting behavior and the transient V-I characteristics, especially in one pulse cycle, would provide useful and essential proofs for understanding the mechanism of PEO process.

The aim of this work is to reveal the growth process of PEO coatings on aluminium alloy by analyzing conducting behavior and V-I characteristics of an aluminium electrode. Therefore, the morphologies and conductive behavior of aluminium alloy electrodes were examined by SEM and capacitance measurement. Meanwhile, the transient V-I characteristics were obtained by automatic signal acquisition system. Further, the reactions and conductive properties in anodic and cathodic regions of one AC pulse were elaborated based on the transient V-I characteristics of an aluminium electrode coated with PEO coatings. Then, the evolution of coating properties was investigated by in-situ monitoring the V-I characteristics in the whole PEO process.

## 2. EXPERIMENTAL

6061 aluminum alloy were chose as specimens with dimensions of  $\phi 38 \times 5$  mm. Before PEO treatment, specimens were ground to 800 grit by SiC papers, degreased in ethanol and cleaned in distilled water. A 2.5 liter double-walled stainless steel cell with cooling system was used as the counter electrode. Electrolyte was composed of 10~20 g/L  $\text{Na}_2\text{SiO}_4$  and 1~5 g/L KOH.

PEO coatings were fabricated at an average constant current density of  $8 \text{ A} \cdot \text{dm}^{-2}$ , frequency of 50 Hz, negative to positive pulse ratio of 1 and for 90 minutes using an AC power equipped with automatic signal acquisition and control system. During PEO process, the transient current and voltage

signals were collected per 33.4  $\mu\text{s}$  and every group data contain four cycles (80 ms) information was recorded per minute.

The surface morphologies of PEO films were examined by FEI Sirion 400NC scanning electron microscopy (SEM). Capacitance measurements of electrode system were conducted using a conventional three electrodes electrochemical cell with the aluminium alloy 6061 as working electrode, a platinum plate as auxiliary electrode and a saturated calomel electrode (SCE) as reference. Capacitance measurements with variable anodic over potential from -1.0~1.0V (SCE) was performed at fixed frequency of 1000 Hz by IM6&Zennium potentiostat in cathodic direction with a scanning rate of 20 mV/s. All experiments were carried out at room temperature.

### 3. RESULTS AND DISCUSSION

#### 3.1. Morphologies characteristics of PEO coatings

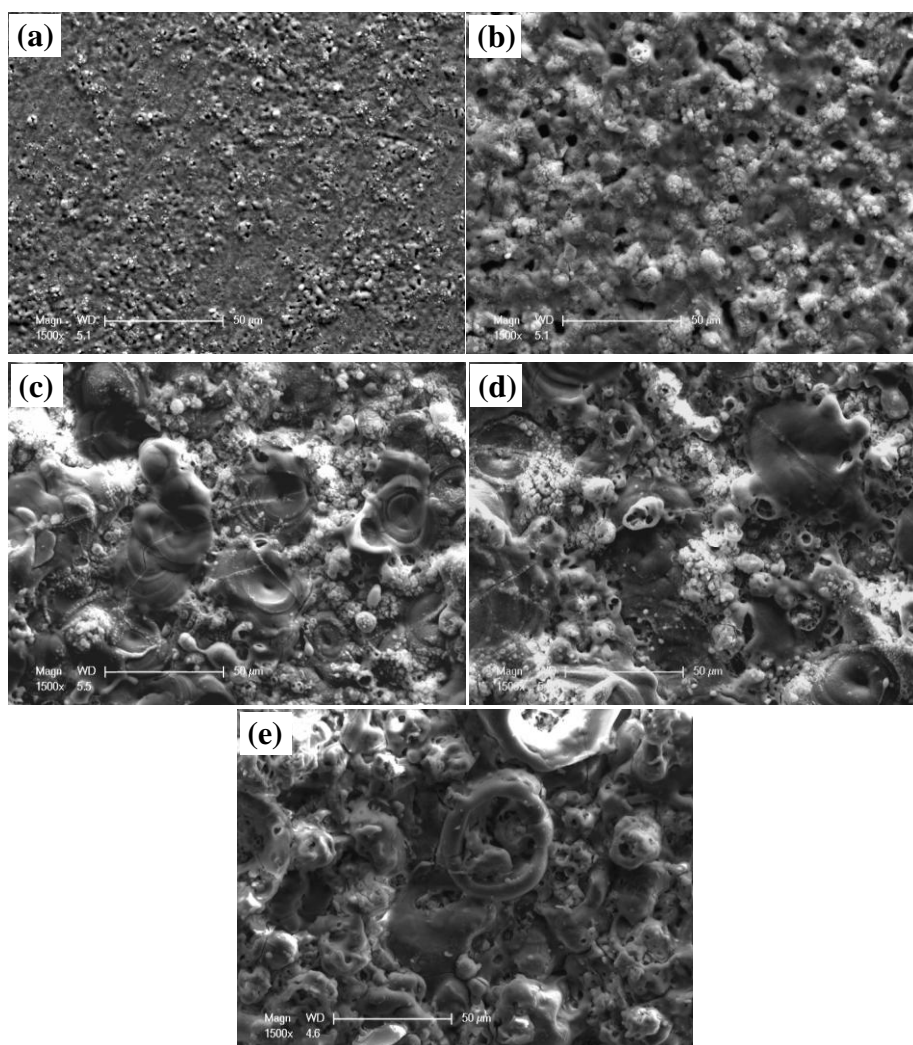


**Figure 1.** Surface morphologies of aluminium alloy 6061 obtained at different PEO stage, (a) 1 min, (b) 10 min, (c) 30 min, (d) 60 min and (e) 90 min.

The surface morphologies of aluminium 6061 samples treated for different time by PEO were shown in Fig. 1. When aluminium electrode was treated for 1 min, there were a few granular products formed on its surface while the coating was very thin that the scratch marks were very evident (Fig. 1a). After 10 min oxidation, the oxide film got uniform and continuous followed by the size of micro pores and sintered particles were all increased (Fig. 1b). As treated time was prolonged to 30 min, there were many plate-like fusion cells (Fig. 1c) resulted from the stronger intensity of spark discharge than that in the initial stage. At the same time, there were many sintered particles around fusion cells which had micro pores in their center. When the treated time was increased continuously (to 60 and 90 min), the morphologies of micro pores and fusion cells were similar as shown in Fig 1d and 1e. But the size of micro pores and fusion cells was increased slightly due to the intensity increase of spark discharge along with thickness increase of PEO coatings.

### 3.2. Conductivity and circuit model of electrode system

The transient voltage/current-time responses in one AC pulse at the first minute under constant average current were shown in Fig. 2. It can be seen that the positive peak current ( $I_+ = 15.3 \text{ mA/mm}^2$ ) was similar to the negative one ( $I_- = -16.2 \text{ mA/mm}^2$ ). While the positive maximum voltage (405 V) was 5 times higher than the negative one (-69 V) (curve II in Fig. 2). This demonstrated that the anodic and cathodic conductive behaviors of the aluminum electrode were different.

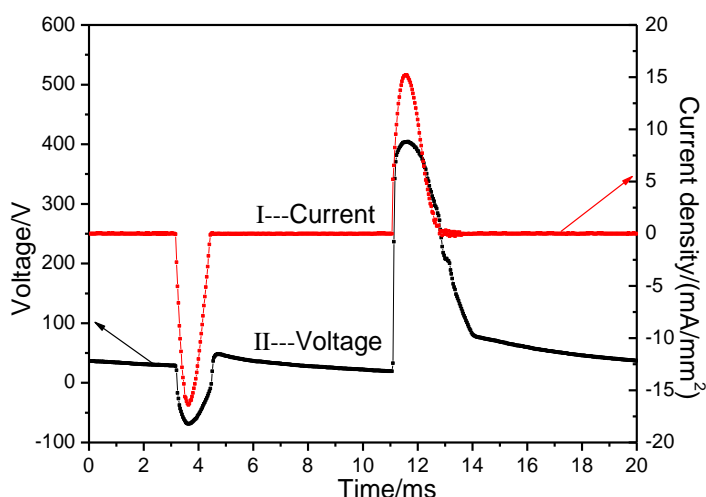


**Figure 2.** The transient current-time (I) and voltage-time (II) responses in the first minute of PEO process of 6061 aluminium alloy in alkaline silicate electrolyte.

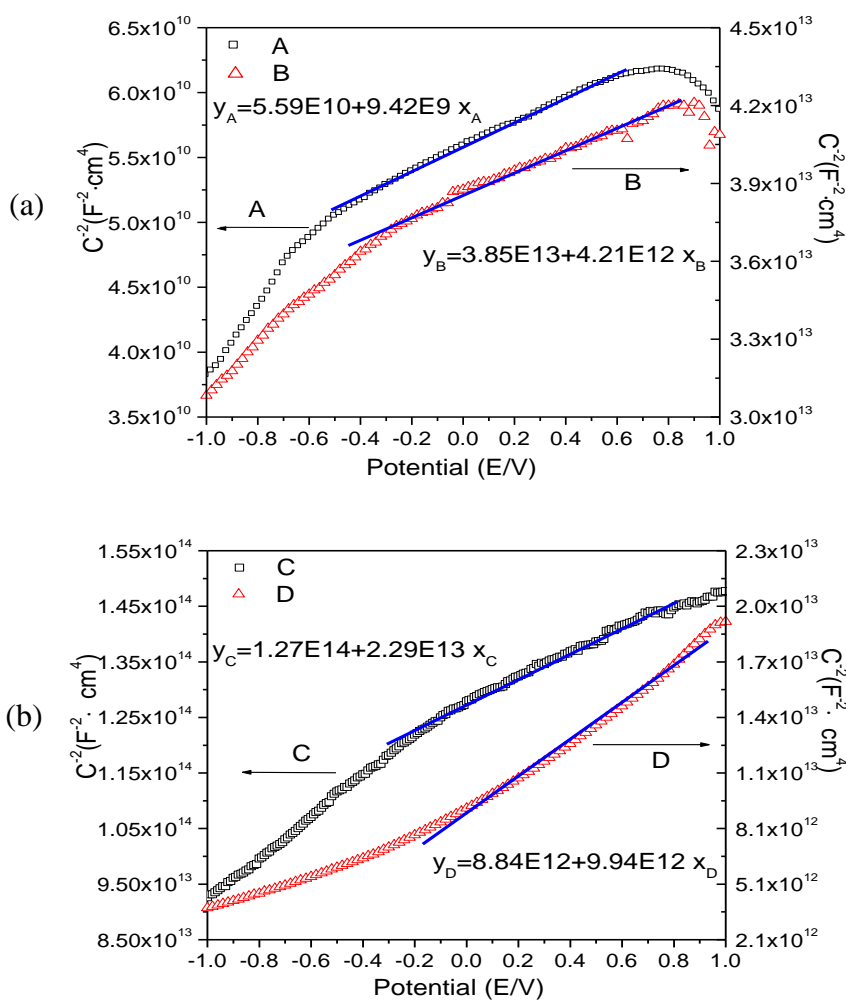
The different voltage-time behaviors in anodic and cathodic branches (shown in Fig. 2) can be explained by the essential conducting properties of valve metals. As some investigations suggested that ceramic barrier layer formed on valve metal surface by PEO treatment prevent transfer of ions and electrons. So, the conductive properties of valve metal electrode with oxide coatings are different from general metal electrode but present some semiconductor properties in electrolyte [13, 16]. Capacitance

measurement based on Mott-Schottky (MS) theory [17, 18] is a conventional technique to probe electronic properties of a semiconducting electrode in aqueous electrolyte. Thus, electronic properties of semi-conductive aluminium electrodes can be analyzed by capacitance measurement, which reflects the effect of the applied potential E on capacitance values, based on equations (1) and (2):

$$\frac{1}{C_{SC}^2} = \frac{2}{\epsilon\epsilon_0 e N_d} \left( E - E_{fb} - \frac{kT}{e} \right) \quad (1) \quad (\text{n-type semiconductor})$$

$$\frac{1}{C_{SC}^2} = -\frac{2}{\epsilon\epsilon_0 e N_a} \left( E - E_{fb} - \frac{kT}{e} \right) \quad (2) \quad (\text{p-type semiconductor})$$

The detailed explanation about the MS measurement can be found in reference [13]. Moreover, the negative slope indicates the electrode has p-type semiconductor properties, while the electrode presents n-type semiconductor property when the slope of MS curves is positive. Furthermore, larger slope of MS curve coincides with lower concentrations of donor or acceptor [18].



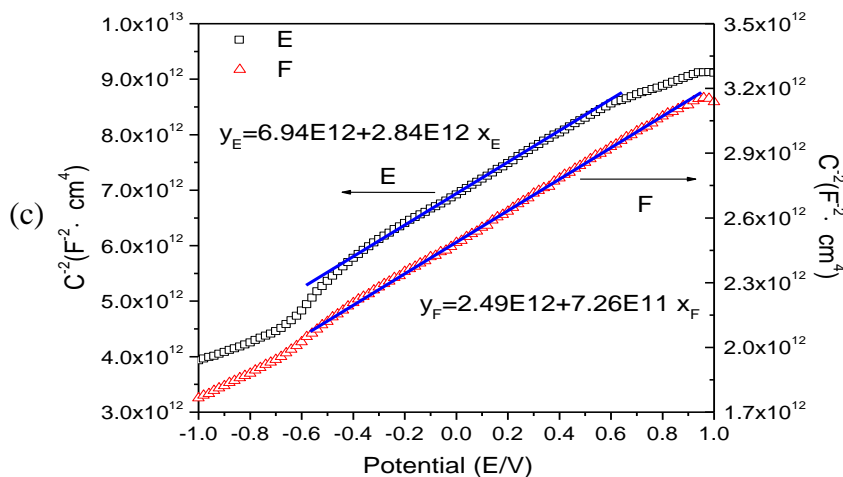


**Figure 3.** Mott-Schottky plots of aluminium alloy 6061 in PEO solution substrate (A) and the sample oxidized for 1 min (B), 10 min (C), 30 min (D), 60 min (E) and 90 min (F).

Fig. 3 showed the MS curves of aluminium electrode with oxide film obtained in different PEO stage. It can be seen that these MS curves all presented positive slope although these PEO coatings had different structure as shown in Fig. 1. Therefore, the aluminium electrodes with and without PEO film all had n-type semiconductor properties and the current transferred in oxide film was mainly conducted by moving of cation interstitials or anion vacancies [19, 20]. The capacitance measurement for aluminium substrate reflected the properties of naturally passive film formed in alkaline silicate electrolyte. While, MS curves of electrodes after PEO treatment reflected the conductive properties of metal substrate and ceramic oxide coatings formed by spark discharge. Simulation of the linear region in MS curves indicated that the slope of MS curves was increased two to three orders of magnitude after the electrodes were oxidized. That is the concentration of donors was decreased evidently due to increase of surface coverage and coating thickness as PEO process prolonged. Otherwise, the slope of MS curves and the donor concentration of PEO coatings obtained at different stage were in the same level although the structure and thickness were different apparently. Therefore, it can be concluded that coating thickness had little effect on the concentration of defects and ions in PEO coatings once dense and uniform coatings were formed under initial spark discharge stage.

The n-type semiconductor properties of electrode system would result in special charge distribution in the interface of metal substrate and oxide coatings. Moreover, the “metal semiconductor junction” coupled by metals and n-type semiconductors was named as “Schottky Barrier Diode, (SBD)”. Thus, a kind of SBD-type structure would be formed by the aluminium electrode and oxide coatings, which had rectification effect and the anodic and cathodic conductive behaviors were different [21, 22]. The aluminium electrode system with SBD-type structure can be figured as the simplified sketch in Fig. 4. Here, the region from line 0 to 0’ was assumed as the original location of the build-in electric field, and the regions from line 1 to 1’ and line 2 to 2’ were the build-in electric field under the effect of positive or negative electric field, respectively. The detailed conductive

behaviors of the aluminium electrode system during PEO process would be systemically presented by the following transient V-I characteristics.

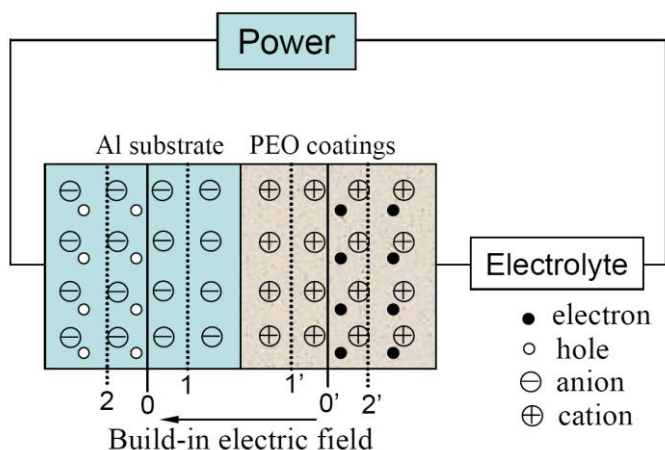


**Figure 4.** Simplified structure sketch of the aluminium electrode system in alkaline silicate electrolyte.

### 3.3. Transient V-I characteristics

The transient V-I curve in the initial PEO process was shown in Fig. 5, which was composed of anodic region ( $U > 0$ ) and cathodic region ( $U < 0$ ). According to the varying direction of voltage, the I-V curve also can be divided into loading (voltage increasing) branch and unloading (voltage decreasing) branch. It can be seen that the anodic region were enclosed by anodic loading and unloading branches, and the cathodic region was approximate linear. The distinction between loading and unloading branches in anodic region illustrated that the anodic process were irreversible.

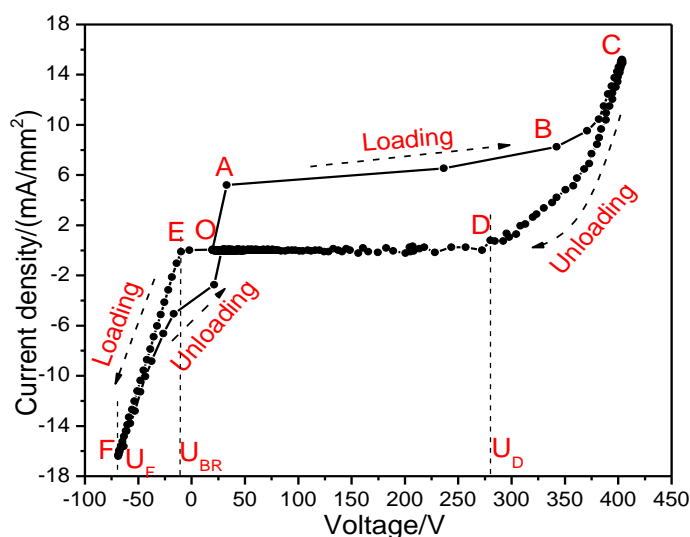
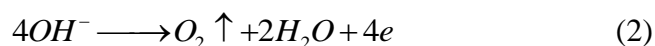


**Figure 5.** The transient V-I characteristics in the first minute of PEO process of 6061 aluminium alloy in alkaline silicate electrolyte.

### 3.3.1 Reaction process in anodic region

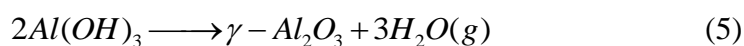
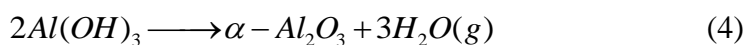
Based on the slope of V-I curve in Fig.5, the anodic loading branch could be divided into three stages: (I) from point O to A, (II) from point A to B and (III) from point B to C. And the anodic unloading branch was composed of two stages between point C to D and D to O.

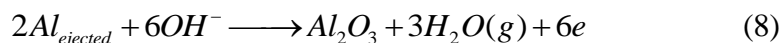
At the beginning of PEO process (stage I), the current was increased rapidly when positive voltage was applied on aluminium electrode. This was because the direction of the external electric field was reverse with that of the build-in electric field of the SBD-type aluminium electrode system under effect of positive voltage. Consequently, the space charges were reduced and the SBD junction was narrowed from region 00' to 11' in Fig. 4. Positive diffusion current from substrate to coatings was formed and sharply increased with the applied voltage getting more positive. Otherwise, anions in electrolyte would transfer toward aluminium electrode rapidly and exchange charges with carriers in coatings once positive electric field was applied. During this stage, the total current across the electrode was sum of the electronic current ( $j_e$ ) and the ionic current ( $j_{ion}$ ). Reactions in this stage were main metal dissolution, oxygen evolution and coatings growth [11]:



As the positive voltage and transport rate increasing (from point A to B in Fig. 5), the concentration of reactants around the electrode increased continuously so that the supplying rate faster than the consumption rate of reactants. Thus, the electric field intensity was increased continuously as more and more excess charges were accumulated in the interfaces of metal/coatings and coatings/electrolyte.

When the electric field intensity was strong enough, electronic avalanche and oxide coatings breakdown would be generated accompanying with numerous spark discharge and high strength anodic leakage current. Here, the current was increased sharply, which coincided with the high slope range from point B to C in Fig. 5. During this stage, the dominant reactions taken place on the aluminium electrode were transformation of anodic oxide to sintered oxide (reactions 4-6) and direct combination of atom Al and O in plasma state under the effect of spark discharge (reactions 7 and 8) [23].





After positive voltage reached the peak value of AC pulse (about 405 V), the electrode process went into unloading stage (from point C to D in Fig. 5). If only the applied voltage on aluminium electrode system was positive enough, the coating growth, spark discharge and sintering reactions still proceeded. But the intensity of electric field and total current were decreased rapidly for existence of the anodic leakage current. At the same time, the concentration of accumulated anions in electrode interfaces was reduced continuously as voltage reducing. Consequently, spark discharge got weak and disappeared finally, and the sintering and plasma reactions were gradually replaced by the electrochemical reactions.

When voltage decreased to point D (about 280 V in Fig. 5), the current of aluminium electrode system closed to zero, which indicated the transition of electronics and ions across PEO coatings was very hard by then. The corresponding voltage ( $U_D$ ) where the current closed to zero was named as the critical conductive voltage. Thus, the electrode system presented capacitor properties and was charged till the end of the unloading stage in anodic region.

### 3.3.2 Reaction process in cathodic region

When a negative voltage was applied on the aluminium electrode, direction of the external electric field was coincided with that of the build-in electric field. Hence, the SBD-type junction was widened from region 00' to 22' in Fig. 4, which reduced the number of carriers crossed junction region and transferred into metal substrate. Therefore, the negative current from oxide film to Al substrate was cut-off and no dependence on the applied voltage in a narrow range ( $U_{BR} < U < 0$ ). This was exhibited as a horizontal line in negative loading branch (from point O to E in Fig. 5). When voltage getting more negative, reverse breakdown would be caused in the SBD-type structure at  $U_{BR}$ . As a result, the negative current was linearly increased with negative voltage increasing from point E to F in Fig. 5. This indicated that the electrode system has constant resistance.

When the applied voltage reached the negative peak value ( $U_F$  in Fig. 5), the negative current decreased almost along the loading branch. During cathodic process, there were some side reactions for the accumulation of cations in interfaces of electrode system, such as hydrogen evolution (reaction 9) or unstable oxide dissolution (reaction 10). There were no redox reactions of coating compositions, though the dissolution of PEO coatings would reduce the resistance of coatings slightly. Thus, there was no evident deviation between the loading and unloading branches in cathodic region.



### 3.4 Growth process of PEO coatings on aluminium alloys

The transient V-I characteristics also can be used to monitor the coatings growth in the whole PEO process. As shown in Fig. 6, these V-I characteristics had similar tendency in one AC pulse cycle during different PEO stage. Compared curves II and III with curve I, the evident changes were disappearance of high slope stage around positive peak voltage. Variations of V-I characteristics during PEO process were determined by the properties of the aluminium electrode system. As PEO treatment time prolonged, PEO coatings was thickened and compacted and the coating resistance was also increased. At the same time, the density of spark discharge was reduced. Thus, the density of anodic leakage current formed by avalanched breakdown was also reduced during PEO process. This made the current slowly increased till the voltage arrived peak value.

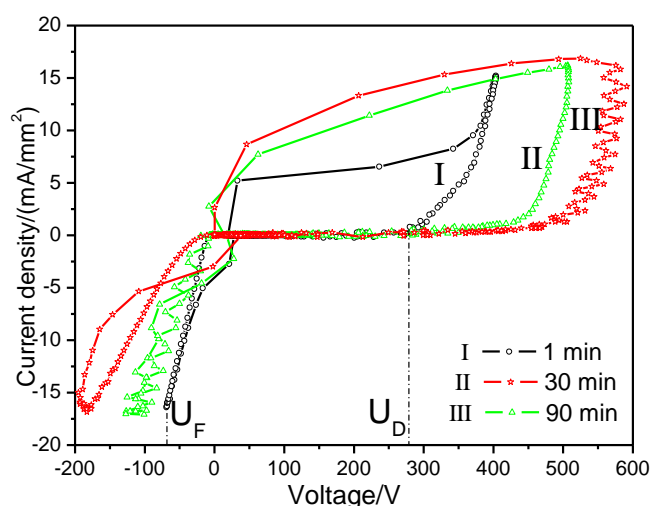


**Figure 6.** The transient V-I characteristics at (I) 1min, (II) 30min and (III) 90min of PEO process of 6061 aluminium alloy in alkaline silicate electrolyte.

The other difference was the area of enclosed anodic region was enlarged and the absolute value of the critical conductive voltage ( $U_D$ ) and the negative peak voltage ( $U_F$ ) was increased as treatment time prolonged. The variations of  $U_D$  and  $U_F$  in the whole PEO process for 90 minute were shown in Fig. 7.

At the initial stage of PEO process, the general anodic oxidation reactions were replaced by plasma reactions and sintered effect after spark discharge occurred. Consequently, the oxide coatings were thickened and the coating resistance was increased quickly due to formation of the ceramic coatings. Thus, the absolute value of  $U_D$  and  $U_F$  was increased rapidly during the initial 10 minute and then they were increased gently.

These results coincided with the MS measurement (in Fig. 3) that the donor concentration lessened rapidly due to resistance increase abruptly in the initial PEO stage. These results indicated that the coating resistance in positive and negative direction was both increased due to thickening and densification of coatings as PEO treatment time prolonged.

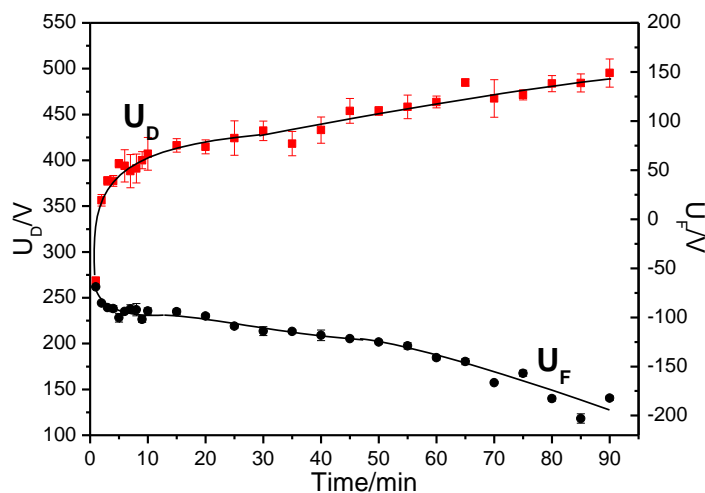


**Figure 7.** Variations of the critical conductive voltage ( $U_D$ ) and the negative peak voltage ( $U_F$ ) with treatment time prolonged in the whole PEO process of 6061 aluminium alloy in alkaline silicate electrolyte.

#### 4. CONCLUSIONS

The surface roughness of PEO coatings was increased as treatment time prolonged and the existence of ceramic oxide coatings make the electrode exhibited n-type semi-conductive properties. The n-type semi-conductive properties built a Schottky barrier diode (SBD)-typed structure with the rectification effect on current, which endowed aluminium electrode system with different conductive behavior in anodic and cathodic region. The transient V-I characteristics indicated that the anodic process were irreversible for existence of redox and sintered effect during PEO process, while the cathodic stage was approximately linear. The transient V-I characteristics in the whole PEO process revealed that the coating resistance in positive and negative directions was both increased nonlinearly as PEO treatment time prolonged. Obviously, the methods and results reported in this study will throw a new light on how to discover the electrochemical reaction mechanism of PEO process of valve metals.

#### ACKNOWLEDGEMENTS

The author would like to thank the financial support of the National Nature Science Foundation of China (Nos: 10772179, 10832011) and China Postdoctoral Science Foundation (20090460536).

#### References

1. A.L. Yerokhin, X. Nie, A. Leyland, A. Matthews, S. J. Dowey, *Surf. Coat. Technol.* 122 (1999) 73
2. A.L. Yerokhin, A. Shatrov, V. Samsonov, P. Shashkov, A. Pilkington, A. Leyland, A. Matthews, *Surf. Coat. Technol.* 199 (2005) 150
3. W. B. Xue, C. Wang, Z. W. Deng, R.Y. Chen, Y. L. Li, T. H. Zhang, *J Phys-Condens Mat.* 14 (2002) 10947

4. G. Sabatini, L. Ceschini, C. Martini, J. A. Williams, I. M. Hutchings, *Mater. Design* 31 (2010) 816
5. H. P. Duan, K. Q. Du, C. W. Yan, F. H. Wang, *Electrochim. Acta* 51 (2006) 2898
6. C. S. Dunleavy, I. O. Golosnoy, J. A. Curran, T. W. Clyne, *Surf. Coat. Technol.* 203 (2009) 3410
7. R. Arrabal, E. Matykina, T. Hashimoto, P. Skeldon, G. E. Thompson, *Surf. Coat. Technol.* 203 (2009) 2207
8. A.L. Yerokhin, L. O. Snizhko, N. L. Gurevina, A. Leyland, A. Pilkington, A. Matthews, *J. Phys. D: Appl. Phys.* 36 (2003) 2110
9. F. Mecuson, T. Czerwiec, T. Belmonte, L. Dujardin, A. Viola, G. Henrion, *Surf. Coat. Technol.* 200 (2005) 804
10. R. O. Hussein, X. Nie, D. O. Northwood, A. Yerokhin, A. Matthews, *J. Phys. D: Appl. Phys.* 43 (2010) 105203
11. A.W. Hassel, D. Diesing, *Electrochem. Commun.* 4 (2002) 1
12. O. E. Linarez Perez, V. C. Fuertes, M. A. Perez, M. L. Teijelo. *Electrochem. Commun.* 10 (2008) 433
13. H. P. Duan, C. W. Yan, F. H. Wang, *Electrochim. Acta*, 52 (2007) 5002
14. E. M atykina, R. Arrabal, A. Mohamed, P. Skeldon, G. E. Thompson, *Corr. Sci.* 51 (2009) 2897
15. Y. J. Guan, Y. Xia, G. Li, *Surf. Coat. Technol.* 22(2008) 4602
16. J. M. Zhao, F. Gu, X. H. Zhao, Y. Zuo. *Acta Phys.-Chim. Sinica*, 24 (2008) 147
17. S. R. Morrison, *Electrochemistry at Semiconductor and Oxidized Metal Electrodes*, New York, 1980
18. M. Metikos-Hukovic, S. Omanovic, A. Jukic, *Electrochim. Acta* 45(1999) 977
19. Y. H. Lin, R. G. Hu, C. J. Lin, *Acta Phys.Chim. Sin.* 21(2005) 740
20. D. D. Macdnald, *J. Electrochem. Soc.*, 148 (2001) B425
21. M. M. Lohrengel, *Mat. Sci. Eng. R.* 11 (1993) 243
22. S. Ikonopisov, *Electrochim. Acta*, 14 (1969) 761
23. L. O. Snizhko, A. L. Yerokhin, A. Pilkington, N. L. Gurevina, D. O. Misnyankin, A. Leyland, A. Matthews, *Electrochim. Acta*, 49 (2004) 2085